Proceedings Paper:

IGBT'S AGEING AND ITS IMPACTS ON THE EM CONDUCTED EMISSIONS

E. Dimech[#1*2], J.F. Dawson[#1]

[#]School of Physics, Engineering and Technology, The University of York, UK

[*]Department of Electronic Systems Engineering, Faculty of Engineering, University of Malta, Malta

[1]evan.dimech@um.edu.mt, [2]john.dawson@york.ac.uk

Abstract — **IGBTs play crucial roles in various power electronic applications, demanding reliability over extended periods. Understanding their failure mechanisms is vital for manufacturers and engineers. This study addresses gaps by correlating IGBT degradation, particularly die-attach and gate oxide contamination, with conducted electromagnetic (EM) disturbances. Accelerated aging was conducted on 600V, 16A IGBTs using a power cycling system, revealing significant changes in static and dynamic parameters. Switching transients showed a slowdown in turn-off, attributed to the experienced degradation. Experimental setups demonstrated a direct link between degradation, switching transients, especially collector current (I_C) turn-off, and reduced conducted EM disturbances.**

Keywords — **IGBTs, Die-Attach Degradation, Gate-Oxide Degradation, Accelerated Aging, IGBTs' Signals Spectral Analysis, Conducted EM Emissions.**

I. INTRODUCTION

Insulated Gate Bipolar Transistors (IGBTs) represent a critical component in power electronic systems, combining the advantageous characteristics of Bipolar Junction Transistors (BJTs) and Metal-Oxide-Semiconductor Field-Effect Transistors (MOSFETs). They are favoured for their ability to handle high voltages while offering efficient on-state capabilities, making them ubiquitous in various applications. However, throughout their operational lifespan, IGBTs are susceptible to numerous degradation and failure mechanisms stemming from diverse factors such as the operational environment (thermal, chemical contamination), the electrical conditions (over-voltage and over-load scenarios), and regular usage-induced aging. These mechanisms can be broadly categorized as semiconductor-related or package-related failures, each posing significant challenges to the reliability and longevity of the device. These will lead to ruptures, lift-off, and cracking of the bond wires, deterioration of the metallization layers, including solder delamination, cracking, and voiding, and degradation of the gate oxide. Notable studies in this domain include the works of Ciappa et al. [1] and Busca et al. [2], which have contributed significantly to identifying and understanding IGBT failures.

A crucial aspect of failure prediction and prevention is the identification of failure precursors, which are events or series of events signalling an impending failure. By monitoring these precursors and detecting deviations from typical behaviour allows for assessing the device's health and taking preventive actions to avoid major failures.. Accelerated aging procedures are commonly employed to induce controlled degradation in IGBTs, which are normally obtained over an extended period. During these procedures, deviations in various parameters are characterized, eventually informing prognostic algorithms that predict the device's remaining useful life. Various research efforts explore a range of IGBT failure precursors, examining both electrical and mechanical factors [3-4]. Abuelnaga et al. provided an extensive review of IGBT failure mechanisms, analysing various failure modes, test setups for controlled degradation, diagnostic parameters, and lifetime modelling techniques [5]. While there is extensive literature on identifying IGBT failure precursors and corresponding prognostic techniques, limited research has explored the correlation between specific IGBT degradation and aging mechanisms and their impact on electromagnetic (EM) emissions. In [6], Chu et al. explored how bond-wire lift-off influences the conducted electromagnetic interference (EMI) of an IGBT module, revealing significant changes in disturbance levels, primarily at the lower frequencies. However, the correlation in higher frequency ranges was less evident, suggesting that changes happening within the IGBT's parasitic elements may have a greater impact on conducted EMI. Feng et al. [7] simulated aging effects on IGBT modules, emphasizing the influence of parasitic capacitances on conducted disturbances. Biswas et al. utilized the near magnetic field to assess the health status of IGBTs, treating the IGBT as a magnetic dipole. This was accomplished using a near-field coil, revealing an overall reduction in interference, particularly at specific frequencies [8]. Moreover, the same authors extended this latter technique to assess the concurrent degradation of multiple IGBTs, by employing a linear array of near-field coils [9].

II. IGBTs ACCELERATED AGEING

In a previous study by the same authors of this study [10], it was shown that the applied accelerated aging procedure, produces measurable alterations in the static parameters of tested IGBTs. In a subsequent study [11], a double-pulse system was developed to characterize the switching dynamics of IGBTs exposed to the same accelerated ageing procedure. The findings demonstrated that the implemented procedure led to a significant slower turn-off. On the other side the turn-on transients experienced only negligible changes. This was

attributed to increased voiding in the die-attach, confirmed through X-ray imagery. This voiding led to elevated junction thermal impedance ($R_{\theta JC}$), which in turn raised the junction temperature (T_J). The elevated temperature under identical operational conditions led to an extended "tailing current" during turn-off after aging. Additionally, modelled changes in parasitic elements due to gate-oxide degradation further contributed to the overall slowdown of the IGBTs. The aging technique, based on Sonnenfeld et al.'s method [12], employed thermoelectric overstress without a heatsink, causing the Device Under Test (DUT) to self-heat and exceeding the maximum junction temperature (T_{JMAX}). The accelerated aging system autonomously maintained the IGBT's case temperature (T_C) within a specified range by controlling the gate signal. Aging proceeded until the DUT latched-up, hence triggering the IGBT's parasitic thyristor structure (loosing gate control), followed by controlled cooling to prevent thermal runaway and hence DUT's destruction. Each IGBT (International Rectifier IRG4BC30KDPBF TO-220 600V/16A) [13], underwent three of the described accelerated aging iterations.

Hence, this study, transcending from a broader study [14], aimed to experimentally determine whether the changes in static and dynamic IGBT parameters, induced by the implemented accelerated degradation procedure, resulted in any measurable and correlatable differences in the EM conducted emissions of an Equipment Under Test (EUT) using a new IGBT compared to the same EUT using the same IGBT, but aged. This entailed developing an experimental setup to measure RF conducted disturbances on both the forward and reverse current paths of the EUT, while concurrently measuring the IGBT's collector voltage (V_C) and collector current (I_C) switching transients to analyse their respective frequency-domain spectra.

III. IMPLEMENTED EM CONDUCTED EMISSIONS TEST SETUP

Fig. 1 illustrates the block diagram of the experimental setup used in this study. The setup centres on a double-pulse test circuit acting as the EUT. This primarily includes a half-bridge circuit switching an inductive load, designed to assess the IGBT's switching dynamics, as detailed in [9]. A mixed domain oscilloscope was employed to acquire the collector voltage (V_C) and the collector current (I_C) during a complete cycle of the double-pulse. Concurrently, the corresponding Fast Fourier Transform (FFT) was performed on-board the oscilloscope, for both signals, to obtain the respective frequency spectra. A programmable signal generator, controlled via custom-made software (developed in National Instruments LabVIEW), generated the double-pulse signal. The initial pulse duration was set at 2.2µs, followed by a 2µs pulse, repeating every 0.1ms at a 6% duty cycle. To prevent self-heating of the IGBT during EM characterisation, a low duty cycle was maintained and the IGBT's case temperature (T_C) was kept at 25°C, monitored via a Type-K thermocouple. These measures aimed to ensure that any detected changes in EM emissions were primarily due to IGBT degradation. In practical applications, larger duty cycles are used, which could cause heating effects and lead to greater EM disturbances. Nevertheless, the primary goal of this study was to measure the changes in conducted EM disturbances resulting from the inflicted degradation of the IGBTs, induced through the implemented accelerated aging procedure, primarily affecting the IGBTs' die-attach and gate-oxide.

According to the Comité International Spécial des Perturbations Radio (CISPR) conducted emissions procedure, all external power cables of the EUT should pass through a Line Impedance Stabilisation Network (LISN). In this setup, due to the availability of only one LISN, only the main power supply input (the DC link voltage) passed through it. Hence, the required auxiliary DC gate drive supply voltage was not passed through a LISN, but was provided directly to the EUT from a Source Meter Unit (SMU) with a valid calibration certificate. The SMU's high precision ensured a relatively constant output impedance, thus guaranteeing the best available degree of repeatability throughout the different experiments. A High Voltage (HV) power supply was utilised to provide the DC link voltage. The output of this power supply was connected via the LISN to the EUT. The NARDA PMM L2-16B, a CISPR compliant LISN, was used, with its RF output connected to a NARDA PMM-EMI Receiver 9010F compliant with CISPR 16-1-1 and MIL-STD-461. This receiver is capable of measuring disturbances, within the 10Hz to 30MHz bandwidth. employing a real-time, gapless, direct conversion EMI measurement based on FFT calculation. Data capture was managed through the PMM Emissions Suite software. Aluminium sheets were utilized to form Vertical and Horizontal Ground Planes (VGP and HGP). These were bolted together via 16 Copper M6 bolts placed every 8cm, for effective electrical connection. The LISN was bolted to the HGP with 3 Copper M6 bolts on each side, ensuring proper grounding. Power cables were fixed to maintain setup consistency across tests on different IGBT samples. The HGP was covered with 5mm clear cast acrylic for safety and electrical isolation. The EUT's placement was standardized, 40cm from the LISN, 50cm from the VGP, 9.5cm above the HGP, and 35cm from the bottom of the table supporting the instrumentation. This is illustrated in Fig 2.

IV. EXPERIMENTAL PROCEDURE

The EUT's DC link voltage was set to 200V DC thus ensuring that it is within the operational range of the LISN's DC voltage. This voltage level, in conjunction with a load inductance of 66µH and an opening pulse duration of 2.2µs, resulted in a test collector current (I_C) of 6.7A. A 20dB 2W 50Ω attenuator was utilized to further protect the input of the EMI receiver. The insertion of the attenuator was characterized across the bandwidth of interest CISPR16-1-1 A and B bands (9kHz-30MHz) using the EMI receiver's internal calibrated RF generator. During the testing campaign, the receiver was set to utilize an "RMS" detector, configured with a hold time of 1ms and corresponding Resolution Bandwidth (RBW) of 1kHz. With these configurations, the receiver managed to scan the bandwidth of interest with 10 seconds.
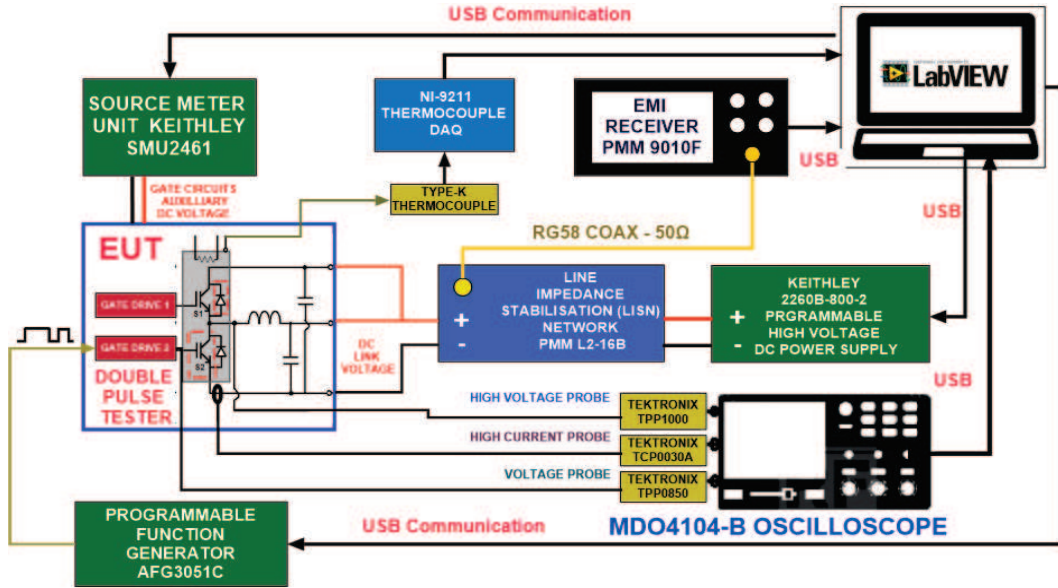
Fig. 1. High level EM conducted emissions, experimental setup.

These settings were chosen as they were deemed optimal when considering the characteristics of the involved signals (discontinuous and pulsed), while also balancing the measurement resolution and test duration effectively. The scan duration played a crucial role, impacting the number of IGBT samples, capable of enduring the entire accelerated aging procedure, which consisted of three age iterations. With longer scans, there was increased power dissipation, heightening the self-heating effect and the likelihood of IGBT failure during conducted emissions testing, particularly as the device deteriorated after each aging iteration. The following procedure was implemented during the EM conducted emissions test campaign to ensure experimental repeatability across different IGBT samples.:

1. Static parameters of the IGBT, including threshold voltage (V_{TH}) and transconductance (g_m), were measured initially, serving as aging indicators and transient modelling parameters.
2. Setup photographs were taken to ensure consistency and repeatability across experiments.
3. An EM emissions scan was conducted with all instruments switched off (apart from the measurement instruments) to measure the noise floor.
4. All instruments were then switched on (but without activating the HV PSU), generating the double-pulse waveform, and noise floors were measured again.
5. The HV PSU was turned on, and EM emissions were measured once the DC link voltage stabilized at 200V. Simultaneously, the transients of the collector voltage (V_C) and collector current (I_C) were recorded, with their respective FFTs via the oscilloscope.

The test campaign involved ten IGBTs. Each IGBT was subjected to three age iterations, and the above measurement procedure was repeated after each age iteration [14].

V. SPECTRAL EVOLUTION OF IGBT SIGNALS AND EM CONDUCTED EMISSIONS DUE TO AGING: RESULTS AND ANALYSIS

The testing campaign focused on the accelerated aging and subsequent characterization of fifteen IRG4BC30KDPBF IGBTs. Out of these, ten IGBTs successfully endured all three aging cycles and the complete characterization process. This section primarily showcases two sets of frequency spectrum results. The first set presents the FFT analyses of the IGBT's collector voltage (V_C) and collector current (I_C) signals. The second group presents the spectra of the conducted emissions measured on the EUT's return line (L_2).
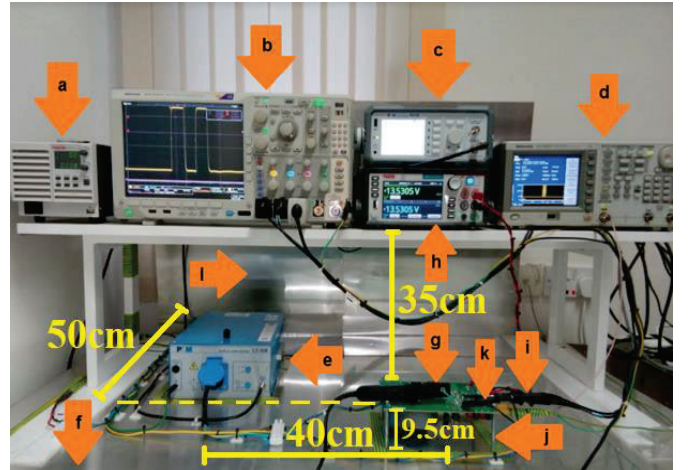

Fig. 2. Experimental setup (a) HV Power Supply (Keithley 2260B-800-2) (b) Oscilloscope (Tektronix MDO4104B-3) (c) EMI Receiver (NARDA PMM 9010F) (d) Double Pulse Generator (Tektronix AFG3051C) (e) Line Impedance Stabilization Network LISN (NARDA PMM L2-16B) (f) HGP (g) High Current Probe (Tektronix TCP003A) (h) Gate Drive Auxiliary Power Supply (Keithley 2461 SMU) (i) High Voltage Probe (Tektronix TPP1000) (j) EUT (k) Low Voltage Probe (Tektronix TPP0850) (l) VGP.

A. Collector Voltage (V_C) Spectral Evolution with Ageing

Fig. 3 displays the measured FFT spectra of the collector voltage (V_C) signal for IGBT Sample 1, for when new and after each aging cycle. The obtained spectra underwent post-processing to identify the spectral peaks. Additionally the least-squares technique was utilised to obtain a polynomial curve, fitting the identified spectral peaks. The obtained plots and the comparative plot of the fitted curves evidences a progressive decrease in the spectral peaks after each aging iteration.

Fig. 4 presents the collective statistics of all ten IGBTs using a box and whisker plot, showing the average spectral magnitude across each 1MHz frequency bin. A comparison is made between the initial state of the IGBTs and after three aging cycles (Age Iteration C). Fig. 5 illustrates a similar plot, but displaying the maximum spectral magnitude across each 1MHz frequency bin. Fig. 4, reveals a general decline in the average spectral magnitude of the collector voltage (V_C) across the 8 to 30MHz frequency range, with the most pronounced reduction occurring between 13MHz and 20MHz.
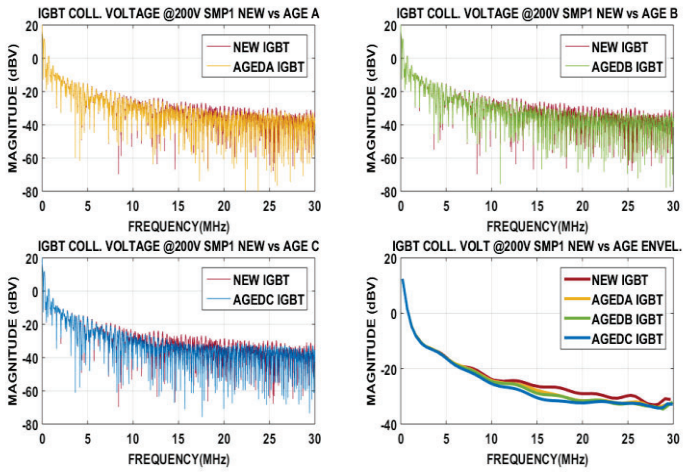

Fig. 3. IGBT Sample 1 Collector Voltage (V_C) FFT Analysis with Aging, comparison of the FFT new with each age cycle, comparison of all the identified peaks fitted curves.
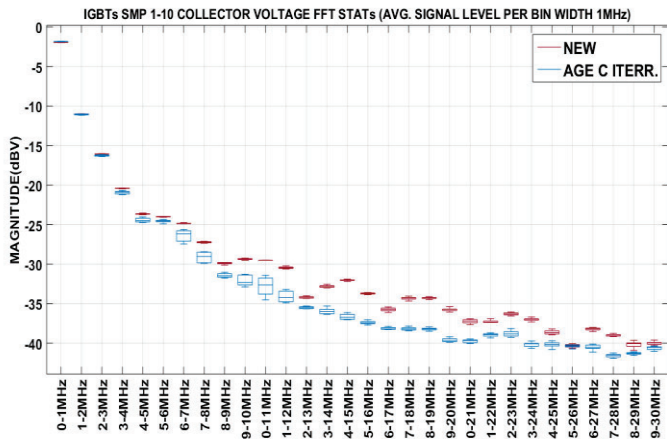

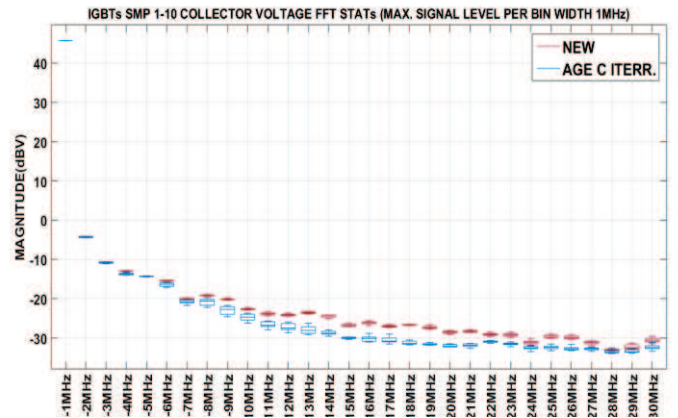Fig. 4. IGBTs 1-10 Aggregated FFT Analysis: Collector Voltage (V_C) Spectral Average Magnitude every 1MHz.

Fig. 5 IGBTs 1-10 Aggregated FFT Analysis: Collector Voltage (V_C) Spectral Peak Magnitude every 1MHz.

The most pronounced decline in the mean average spectral magnitude of the collector voltage (V_C) signal, occurs in the 14MHz-15MHz frequency bin, reflecting a substantial 14.5% decrease. None of the frequency bins manifested an increase in average collector voltage (V_C) spectral magnitude. Furthermore, as demonstrated in Fig. 5, there is an overall decline in the measured maximum spectral magnitude of the collector voltage (V_C) signal, with the most significant reduction appearing between 12MHz and 21MHz. The 12MHz-13MHz frequency bin, revealed the largest maximum spectral magnitude mean percentage decrease of 18.6%.

B. Collector Current (I_C) Spectral Evolution with Ageing

Fig. 6 presents the FFT spectra of the collector current (I_C) signal for IGBT Sample 5, both when the IGBT was new and after successive aging cycles. Following the approach in Section V(A), post-processing identified the key spectral peaks and fitted polynomial curves, revealing a consistent overall reduction in these peaks throughout the aging process. Fig. 7 shows the aggregated spectral data for the current transients (I_C) transients from all ten IGBTs, highlighting the average spectral magnitude within each 1MHz frequency bin..
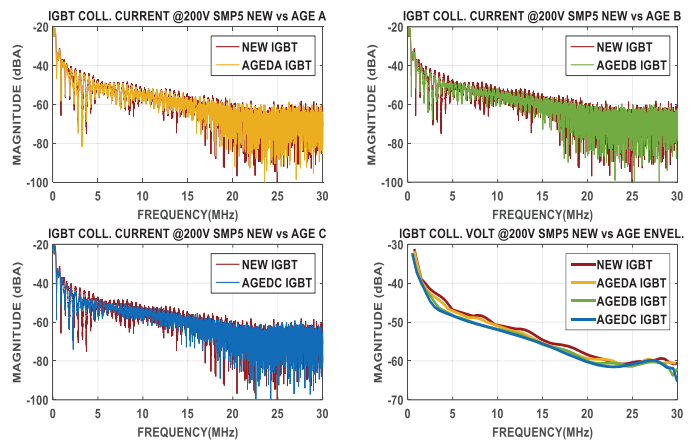

Fig 6. IGBT Sample 5 Collector Current (I_C) FFT Analysis with Aging, comparison of the FFT new with each age cycle, comparison of all the identified peaks fitted curves .

This indicates that there was an overall decrease in the average spectral magnitude across the 1MHz to 20MHz bandwidth after aging., with the most notable decrease observed in the 1MHz-2MHz frequency bin (7.6% decrease). However, there was a corresponding increase in the average spectral magnitude for four frequency bins (3-4MHz, 7-8MHz, 8-9MHz, and 12-13MHz).

Fig, 8 presents a similar plot, illustrating the combined spectral analysis of the maximum magnitude across each 1MHz frequency bin. This revealed a decrease in the spectral maxima across the 2MHz to 20MHz bandwidth. The most significant reduction occurred in the 4MHz-5MHz bin, with a corresponding mean percentage decrease of 7.7%. Even above 20MHz, a decrease in maximum spectral content was observed, albeit less prominently.
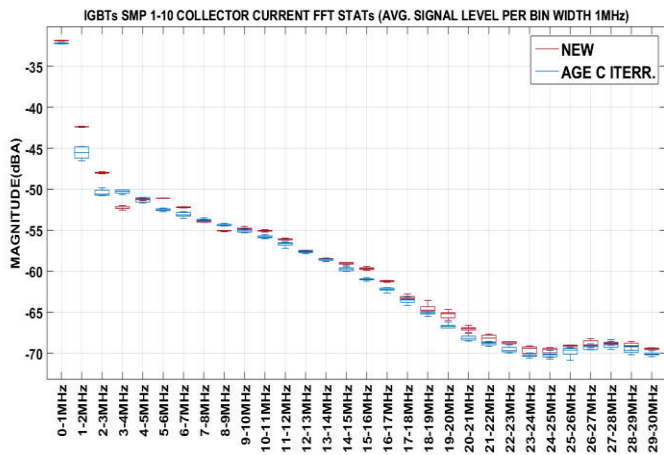

Fig. 7 IGBTs 1-10 Aggregated FFT Analysis: Collector Current (I_C) Spectral Average Magnitude every 1MHz..
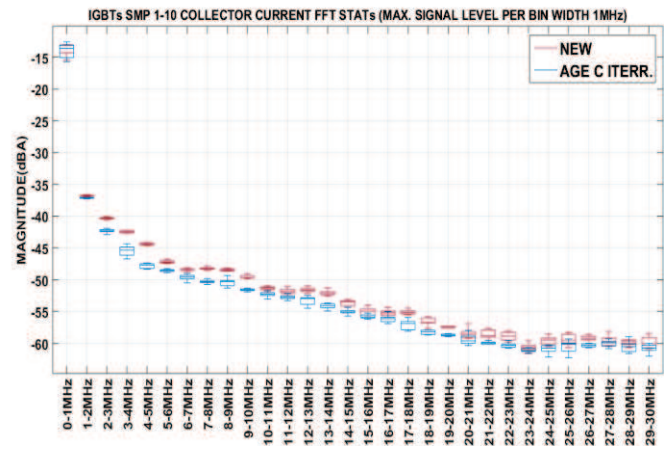

Fig. 8 IGBTs 1-10 Aggregated FFT Analysis: Collector Current (I_C) Spectral Peak Magnitude every 1MHz..

C. *EM Conducted Emissions Evolution with Ageing*

A parallel spectral analysis, mirroring the one described in Sections V(A & B), was undertaken on the measured EM conducted emissions. All analyses covered the same bandwidth of interest, specifically the 9kHz-30MHz range, which reflects the CISPR16-1-1 conducted emissions A

and B bands. This section delves into the analysis of how the spectral characteristics of the measured disturbances on the return line (L_2) of the EUT, changed during the implemented accelerated aging procedure. Fig. 9 illustrates the progression of the measured conducted disturbances for IGBT Sample 3, including the applied post-processing. These results demonstrate a consistent and progressive decline in the power levels of the conducted emissions' spectral maxima across the entire bandwidth of interest. Conversely, there is an overall progressive increase in the spectral minima within this bandwidth as well. This suggests that the accelerated aging process is also contributing to increased power levels at certain frequencies.
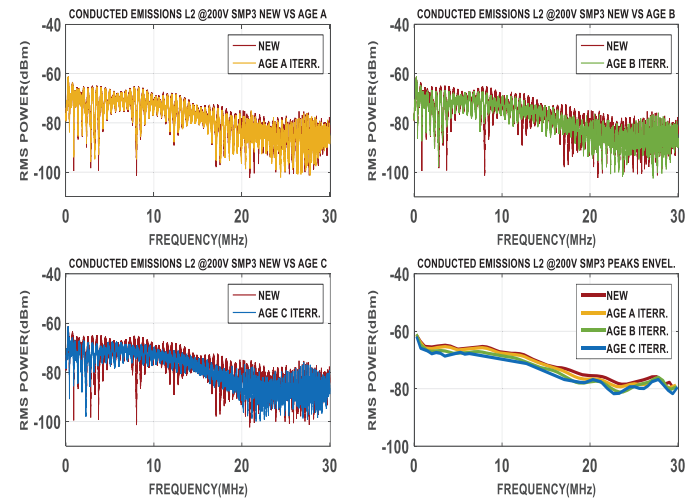

Fig. 9 IGBT Sample 3 EM Conducted Emission Analysis with Ageing, comparison of the emissions new with each age cycle, comparison of all the identified peaks fitted curves .

Fig. 10 and Fig. 11 illustrate the combined spectral analysis of the EM conducted emissions on the return line (L_2) from all ten IGBTs, displaying the average and peak spectral magnitudes across each 1MHz frequency bin, respectively. The results, which indicate a general decrease in peak power levels of conducted emissions, align with the findings from the spectral analysis of collector voltage (V_C) and collector current (I_C). These analyses revealed reductions in spectral peaks within specific frequency ranges (V_C: 12MHz to 21MHz; I_C: 2MHz to 20MHz), reflecting similar changes in the EM conducted emissions within the same bandwidths. This is particularly evident in Fig. 11, which shows a general decrease in the spectral peaks of EM conducted emissions across the entire bandwidth of interest. Fig. 10 shows a general reduction in average spectral power post-aging across most frequency bins, with the largest mean reduction occurring within the 22MHz-23MHz frequency bin, exhibiting a mean percentage decrease of 6.1%. Conversely, four bins (3-4MHz, 7-8MHz, 8-9MHz, and 12-13MHz) displayed increases in average spectral power after accelerated aging, with respective mean percentage increases of 2.5%, 0.2%, 2.5%, and 1.1%. These increases align with the frequency bins that showed a rise in the collector current (I_C) transients average spectral magnitude analysis as depicted in Fig. 7.
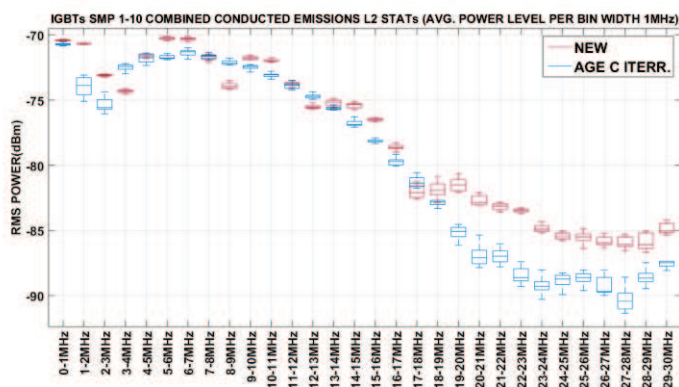
Fig.10 IGBTs 1-10, Aggregated Analysis of Conducted Emissions, Average Spectral Power every 1MHz.
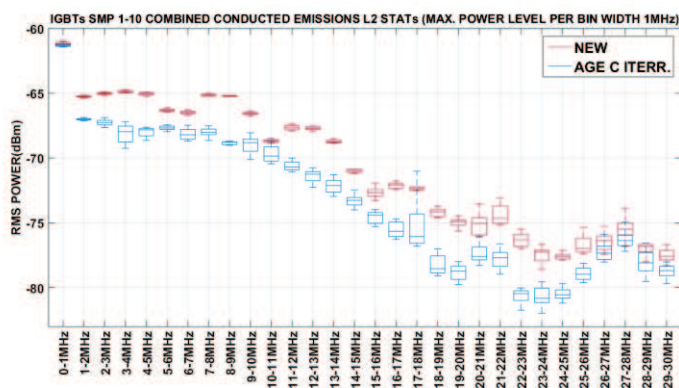

Fig.11 IGBTs 1-10, Aggregated Analysis of Conducted Emissions, Peak Spectral Power every 1MHz.

VI. CONCLUSION

This study sought to identify any measurable deviations in conducted EM disturbances between an EUT employing a new IGBT and the same EUT employing the same IGBT after being subjected to accelerated degradation. The employed accelerated aging process was marked by void formation in the die-attach layer, which raised the IGBT's junction temperature (T_J) due to hindered thermal path. Moreover this aging procedure produced measurable changes in the IGBT input, due to gate oxide degradation. As a result, there was a noticeable slowdown in the turn-off transients of both the collector current (I_C) and collector voltage (V_C), leading to increased power dissipation during turn-off. This degradation was primarily indicated by a prolonged turn-off "tail collector-current" and changes in the IGBT's parasitic elements, primarily the collector-gate capacitance (C_{CG}) [14]. Conversely, the turn-on transients of the IGBTs remained largely unaffected.

Spectral analysis showed a progressive decrease in the magnitude of spectral peaks for both the collector voltage (V_C) signal and collector current (I_C) signal as the IGBTs aged. Additionally, this latter signal demonstrated a measurable increase in average harmonic magnitude within specific frequency bands. These alterations were found to correspond with changes in the EM conducted emissions from the EUT. A progressive reduction in the peaks of conducted emission disturbances was observed as the IGBTs aged. Moreover, the measured EM conducted emissions exhibited an increase in average harmonic power within frequency bands that aligned with increases in the collector current (I_C) average spectral magnitude. Therefore, a degraded IGBT's die-attach resulting in reduced power dissipation, in conjunction with gate oxide contamination, leads to measurable reductions in the EM conducted emissions of an EUT, using such an aged IGBT, compared to an EUT with a new IGBT. These reductions are largely attributed to the general slow-down of the IGBT's turn-off transients, in particular to the collector current (I_C) turn-off.

REFERENCES

[1] M. Ciappa, "Selected failure mechanisms of modern power modules," Microelectronics Reliability, vol. 42, no. 4-5, pp. 653-667, May, 2002..

[2] C. Busca, R. Teodorescu, F. Blaabjerg, S. Munk-Nielsen, L. Helle, T.Abeyasekera, and P. Rodriguez, "An overview of the reliability prediction related aspects of high power IGBTs in wind power applications," Microelectronics Reliability, vol. 51, no. 9-11, pp. 1903-1907, Sep./Nov. 2011.

[3] A. Ginart, M. Roemer, P. Kalgren, and K. Goebel, "Modeling Aging Effects of IGBTs in Power Drives by Ringing Characterization," in IEEE International Conference on Prognostics and Health Management, 2008.

[4] D. W. Brown, M. Abbas, A. Ginart, I. N. Ali, P. W. Kalgren, and G. J. Vachtsevanos, "Turn-off time as an early indicator of insulated gate bipolar transistor latch-up," IEEE Trans. Power Electron., vol. 27, no. 2, pp. 479–489, Feb. 2012.

[5] A. Abuelnaga, M. Narimani and A. S. Bahman, "A Review on IGBT Module Failure Modes and Lifetime Testing," in IEEE Access, vol. 9, pp. 9643-9663, 2021.

[6] C. Chu, C. Dong, M. Du, X. Zhou and Z. Ouyang, "Aging Monitoring of Bond Wires Based on Differential Mode Conducted Interference Spectrum for IGBT Module," in IEEE Transactions on Electromagnetic Compatibility, 2021.

[7] Feng Q.P, Lin Y.W, K L Jin, J Q Zhang, X Q Li and Q F Wang, "The Influence of IGBT Aging on the EMI of Traction Converter", Journal of Physics: Conference Series, Volume 1619, 13th International Conference on Computer and Electrical Engineering 31 July - 2 August 2020, Beijing, China.

[8] R. Biswas, A. Routray, S. Sengupta, M. Pramanik and A. K. Gupta, "EMR signature analysis for health monitoring and early stage fault diagnosis of IGBT," IECON 2017 - 43rd Annual Conference of the IEEE Industrial Electronics Society, Beijing, China, 2017, pp. 5043-5048

[9] R. Biswas and A. Routray, "Application of EMR Signature in Health Assessment and Monitoring of IGBT-Based Converters," in IEEE Transactions on Power Electronics, vol. 35, no. 2, pp. 1899-1906, Feb. 2020.

[10] E. Dimech and J. F. Dawson, "Electrical Parameters Characterization of Aged IGBTs by Thermo-Electrical Overstress," IECON 2018 - 44th Annual Conference of the IEEE Industrial Electronics Society, Washington, DC, USA, 2018, pp. 5924-5929.

[11] E. Dimech and J. F. Dawson, "Switching Parameters Characterization of Aged IGBTs by Thermo-Electrical Overstress," IECON 2019 - 45th Annual Conference of the IEEE Industrial Electronics Society, Lisbon, Portugal, 2019, pp. 4648-4653.

[12] G. Sonnenfeld, K. Goebel, and J. R. Celaya, "An agile accelerated aging, characterization and scenario simulation system for gate controlled power transistors," in IEEE AUTOTESTCON, 2008, pp. 208-215.

[13] "International rectifier IRG4BC30KDPbF datasheet," [Online]. Available: www.infineon.com/dgdl/irg4bc30kdpbf.pdf Last Accessed: 25/11/2023.

[14] Dimech, Evan (2022) Insulated Gate Bipolar Transistor's Ageing And Its Impacts On The Electromagnetic Conducted Emissions. PhD thesis, University of York. Available: https:/etheses.whiterose.ac.uk/30715. Last Accessed: 15th May 2024.